Title

Engineering an elastic and tough hydrogel for load-bearing tissue replacement

Author

Budiman, Annabella

Publication Date

2023

Peer reviewed|Thesis/dissertation

UNIVERSITY OF CALIFORNIA

Los Angeles

Engineering an elastic and tough hydrogel for load-bearing tissue replacement

A thesis submitted in partial satisfaction of the requirements for the degree

Master of Science in Chemical Engineering

by

Annabella Budiman

2023

ABSTRACT OF THE THESIS

Engineering an elastic and tough hydrogel for load-bearing tissue replacement

by

Annabella Budiman

Master of Science in Chemical Engineering

University of California, Los Angeles, 2023

Professor Nasim Annabi, Chair

Hydrogels have been extensively used in tissue engineering applications as they provide versatility in structure and physical properties, which can mimic properties of native tissues. However, most hydrogels exhibit weak compressibility, stretchability, and tend to swell and degrade, which opposes their functionality to be implanted for long periods of time inside the body. Here, we present a strategy to produce macroscopically porous, tough, and elastic poly(vinyl)alcohol (PVA)-based hydrogels using a synergic freeze-thawing and salting-out method that can prepare scaffolds for different load-bearing tissues such as tendons, cartilages, and intervertebral disks. Hydration with inorganic and organic ions actively controlled the stability of the PVA macromolecule and facilitated the formation of micro-structured frameworks with tunable porous structures. The engineered hydrogels showed Young's modulus in range of 116-500 kPa and compressive modulus between 1-5 MPa, comparable to natural load-bearing tissues. In addition, 10% swelling and degradation rate up to 2 months indicated long-term material stability. With the

presence of a quaternary ammonium salt, the engineered hydrogel demonstrated excellent antibacterial property exhibited *in vitro* using both Gram-positive and Gram-negative bacteria. Meanwhile, cytotoxicity the materials were assessed *in vitro* with human lung fibroblast cells which showed >95% cell viability and proliferation over 7 days of culture. Our novel material which is formed by freeze-casting and salting out techniques and tested in biological environments proves itself to be translatable for load-bearing tissue applications.

The thesis of Annabella Budiman is approved.

Panagiotis D. Christofides

Thaiesha Andrea Wright

Nasim Annabi, Committee Chair

University of California, Los Angeles

2023

TABLE OF CONTENTS

LIST OF FIGURES

ACKNOWLEDGEMENTS

I would not be the person I am today without the people I've met and worked with. First, I would like to thank my advisor, Professor Nasim Annabi, for her guidance and support during the course of my research and time as a Masters student, as well as Professor Panagiotis Christofides and Professor Thaiesha Wright for reviewing my thesis. I have also learned a great deal about research and writing with the guidance of Avijit Baidya, my mentor and manuscript co-author, who has taught me great advice about laboratory research, writing skills, academia and life. I hope you are achieving great big things as a professor in India. I would also thank my peers, Saumya Jain (my Bacteria Mommy) and Yavuz Oz, for their assistance and guidance in several experiments such as bacteria, cell study and SEM imaging as I believe deeply in collaboration among peers to foster great scientific achievements and relationships among fellow scientists. I also appreciate the friendships I made in the Annabi lab and UCLA CBE Department, the true "homies" I fostered relationships inside and outside lab during my time as a MS student.

Last of all, I'd like to thank my parents for their continuous support and encouragement on my academic and career pursuits throughout my life. I love you always.

CHAPTER I. INTRODUCTION

Hydrogel-based biomaterials are three-dimensional (3D) crosslinked polymeric networks, with extracellular matrix resembling mechanophysical properties, which are intensively studied as scaffolds for tissue engineering applications[1], matrices for drug delivery[2], tissue adhesives and sealants[3, 4], implantable devices[5] and more. Despite the body's self-healing ability, the extent of tissue repair depends on the severity of the injury or disease and the tissue types, which may require tissue replacement if the condition is too severe. For instance, mature articular cartilage has poor self-healing properties due to the low cell density and avascular nature, demanding the need for implantation or a tissue-like scaffold to support the regeneration.[6] Similarly, degeneration of the intervertebral disk (IVD), which is primarily caused due to the narrowing of the disk height in the lower lumbar segment, often requires surgical interventions for spinal fusion and total disc replacement.[7] In most of the cases, materials used for these therapeutic procedures are integrated with metals or alloys, which can be expensive, prevent motions, and significantly result in the post-surgical complications.[8] For instance, Charite®, activL® and Prodisc®-L are FDA-approved artificial disk replacements for IVD. However, these metal IVD implants increase the risk of injury and degeneration due to their greater yield stress under flexion load, reduced motion-range, and increased facet load.[9] Therefore, as an alternative to these metal integrated implants, it is vital to engineer tough, strong and non-swellable biomaterials that can restore the mechanical function of damaged tissues.

Engineering hydrogels for regeneration of the load-bearing tissues involves designing molecular interactions to introduce tissue-required tunable mechanics and multifunctional physio-chemical properties[10, 11]. However, due to several persistent issues including lack of structural integrity,

uncontrollable swelling, and inadequate mechanical strength, clinical applicability of these hydrogels as implants, which demand high load and large deformation, remains restricted[12]. For instance, hydrogels become mechanically weak and fragile upon swelling in physiological conditions[13]. In addition, high swelling of the hydrogel-based implants may cause pressure on the surrounding tissues. Furthermore, insufficient cohesiveness within the molecular networks result in fragmentation and quick degradation of the hydrogels, increasing the possibility of post-treatment medical coomplications[14]. Therefore, designing hydrogel networks with minimal swelling and controlled degradation while maintaining its toughness and structural strength is essential for their long term stability and function as implants inside the body.

Tough hydrogels are often designed with double networks[15, 16] , interpenetrating multi-networks[17], slide-ring crosslinking[18, 19], and micellar copolymerization[20] in order to harness durable mechanical strength and toughness. Despite the focus on fine tuning molecular interactions, these hydrogels fail to provide natural load-bearing tissue-like extreme mechanical properties (i.e., tendons, muscles) due to the absence of hierarchical structures across multiple length scales.[21] To address this limitation, tough and strong hydrogels were designed with micro/nano-scaled structural architecture, which enabled energy dissipation during their deformations.[22, 23] For instance, polyampholyte hydrogels were integrated with woven glass fiber fabric that improved the interfacial molecular interactions in the hydrogel network and introduced superior strength and toughness.[24, 25] However, these tough biomaterials lack stretchability, ductility, and adequate water retention or storage required to mimic the naturally flexible and tough tissues.

To address these limitations and expand the applications of hydrogel for different biomedical applications, recently tough and strong hydrogels have been synthesized by introducing a dual effect, freeze-casting followed by salting-out.[26, 27] Mechanistically, while freeze-casting of polymeric solution incorporated crystalline domains, salting-out introduced micro/nano-fibril network to strengthen and toughen the hydrogel network. The mechanism of salting-out, known as Hofmeister effect, are well studied in protein precipitation[28], crystallization[29], and colloidal assembly[30]. By using a salting-out mechanism, the fabrication of an ultra tough hydrogel network was demonstrated, where ion-specific interactions with frozen hydrophilic polymer chains at molecular level modulated the mechanical properties of the engineered hydrogels.[12, 31] In those cases, poly(vinyl alcohol) (PVA) is used to engineer these tough hydrogels due to its amphiphilic nature. With both hydrophobic (CH_2-CH_2) backbone and hydrophilic (-OH) side-groups, PVA macromolecules could both introduce crystalline regions in the hydrogels as well as facilitate reorganization upon interactions with different ions. This enabled the tunability in mechanical, structural, and physical properties of the resulting hydrogel. Furthermore, PVA is a biocompatible, nontoxic, and FDA approved macromolecule, which broadens its application in medicine.[32] For instance, PVA-based hydrogels networks were integrated with bacterial cellulose nanofiber to design a strong hydrogel that could be used for the replacement of damaged cartilage.[33] However, in this case, due to the absence of a robust micro/nano-scaled structural architecture, the engineered hydrogel lacked adequate stretchability and compression modulus, which is of utmost importance in designing mechanically versatile hydrogel materials.

Considering the unmet need for designing tough and elastic hydrogels for various tissue engineering applications, herein, microporous hydrogel constructs based on PVA were developed

using the salting-out (Hofmeister effect), which controlled the molecular level interactions between PVA and organo-inorganic ions, choline bicarbonate and sodium bicarbonate. Mechanistically, the reduced ion-hydration of organic ion with hydrophobic quaternary ammonium functionality stabilized the solvated PVA macromolecules which facilitated the formation of anisotropic porosity in the hydrogel constructs. Moreover, by changing the organo-inorganic ion ratios, the macroscopic structural skeletons of the hydrogels were tuned which modulated the hydrogels' mechanical properties. Overall, the synergistic effects of freeze-thawing and salting-out process with the chemical microenvironment architected the structural framework of the hydrogels, which permitted the combination of exceptional compressibility, modulus, strength, and toughness all in one platform. Furthermore, the presence of organic ions from the quaternary ammonium group enhanced the resulting hydrogel with antimicrobial resistance. Altogether, the engineered tough and elastic hydrogels with tunable physical properties have potential to be used for diverse biomedical applications, especially for implants designed as natural load-bearing tissues.

CHAPTER II. MATERIALS AND METHODS

2.1 Materials

Poly(vinyl alcohol) (MW: 89000-98000) and choline bicarbonate (~80% in H_2O) was purchased from SigmaAldrich. Sodium bicarbonate ($NaHCO_3$) and Dulbecco's phosphate buffered saline (DPBS) was purchased from ThermoFischer Scientific. Collagenase type II was purchased from Gibco. 6, 12 and 24-well Polystyrene Tissue Culture Plate with lid were purchased from CELLTREAT Scientific.

2.2 Preparation of Hydrogel

To synthesize hydrogel, initially 10 g PVA (Sigma) was dissolved in 100 mL deionized water at 150°C to obtain a 10 %(w/v) PVA solution. Hereafter, PVA solution was pipetted into well plates to develop disk shaped hydrogel via three freeze-thaw cycles. Each cycle consisted of treatment at -80°C for 60 min followed by treatment at 25°C for 30 min. To induce crosslinking in the hydrogel network, as prepared PVA disks were immersed in a 3M ionic solution for 24 h prepared with different ratios of a 3M choline bicarbonate and a 3M $NaHCO_3$ solutions. A 3M choline bicarbonate and 3M $NaHCO_3$ solution was prepared by dissolving 15.4 mL of choline bicarbonate and 6.3 g of $NaHCO_3$ in 25 mL of deionized water, respectively. Meanwhile, to prepare 25/75 hydrogel, 25% of 3M $NaHCO_3$ was mixed with 75% of 3M choline bicarbonate solution where the PVA hydrogel will be soaked for 24 h. Similarly, to prepare 50/50 and 75/25 hydrogel, 50% of 3M $NaCO_3$ and 50% of 3M choline bicarbonate, and 75% of 3M $NaHCO_3$ and 25% of 3M choline bicarbonate were mixed, respectively where the PVA hydrogel will be soaked for 24 h. After 24 h of freeze-soaking, excess ions absorbed on the PVA hydrogel was removed by washing the ion-

crosslinked hydrogels with deionized water for multiple times and stored at 4°C until they were used.

2.3 Mechanical characterization

2.3.1 Compression test

PVA hydrogels were prepared by pouring 1 ml of 10% PVA solution in 24 well plate, which underwent 3 freeze-thaw cycles and soaked in the salt solutions for 24 h. Hereafter, the sample was placed in between the compression plates of an Instron 5944 mechanical tester and compressed at a rate of 1 mm/min until mechanical failure. Compression data was recorded using a Bluehill Universal software. Compressive modulus was taken as the slope of the linear portion of the stress vs. strain curve. For the Cyclic compression test, the samples were compressed up to 50% at a rate of 1 mm/min for 10 cycles. Energy loss was calculated at the 2nd, 5th and 8th cycle using the following equation where the loading curve occurs when the sample is compressed, and the unloading curve occurs when the sample is decompressed (Eq. 1). (N=5)

$$Energy\ loss\ (\%) = \frac{area\ under\ loading\ curve - area\ under\ unloading\ curve}{area\ under\ loading\ curve} \times 100\% \quad \textbf{(1)}$$

2.3.2 Tensile test

For tensile tests, as synthesized samples were cut into rectangular shape of 4 cm × 1 cm and placed in between two layered paper tape using super glue. Hereafter, the ends of the tape were clamped to both ends of an Instron 5944 mechanical tester to record characteristics and the data was collected using Bluehill Universal software. Samples were pulled to failure at a strain rate of 1 mm/min. Ultimate strength was taken at the maximum stress the disk can endure without mechanical failure. Stretchability was taken at the maximum strain the disk can endure before

failure. Toughness was taken at the area under the stress vs strain curve before failure. Young's modulus was taken as the slope of the initial linear portion of the stress vs. strain curve at 6 to 10% maximum strain. (N=5)

2.3.3 Swelling ratio

For swelling study, as synthesized hydrogels were shaped into semicircle with a diameter of 0.5 cm and submerged in DPBS at 37°C for 72 h. The swelling ratio was calculated using the following equation (Eq. 2), where Wo is the dry mass reported after sample preparation and Wi is the wet mass measured at predetermined time points. (N=4)

$$Swelling\ ratio\ (\%) = \frac{W_o - W_i}{W_o} \times 100\% \qquad \textbf{(2)}$$

2.3.4 Degradation rate

For degradation test, hydrogels were prepared in semicircle shape and submerged in 2 U/mL collagenase type II solution at 37°C for 12 weeks. The collagenase solution was refilled every 3-5 days to ensure that the samples were still fully submerged. The degradation rate (N=4) was calculated using the following equation (Eq. 3), where Wo is the dry mass reported after sample preparation and Wi is the wet mass measured at predetermined time points.

$$Degradation\ rate\ (\%) = \frac{W_o - W_i}{W_o} \times 100\% \quad \textbf{(3)}$$

2.4 Antibacterial test

2.4.1 Bacteria survival test

Bacterial survival test was conducted using *Staphylococcus aureus* (gram-positive) and *Pseudomonas aeruginosa* (gram-negative) bacteria strains. *S. aureus* was first cultured using a

streak plate method on Tryptic Soy Agar (TSA) plates, whereas *P. aeruginosa* was cultured using Luria-Bertani (LB) agar plates. Both TSA and LB agar plates were incubated at 37°C overnight. The bacteria solution was diluted to $1x10^8$ CFU/mL using optical density (OD) measured at 625 nm wavelength using a BioTek Eon Microplate Spectrophotometer. The hydrogels were prepared with 3 freeze-thaw cycles and soaked in different ratios of choline bicarbonate and sodium bicarbonate solutions (100/0, 25/75 and 75/25) for 24 h. The samples were washed with deionized water, sterilized under UV light for 10 min and further used for the antibacterial studies. Once the OD was within 0.06 to 0.08, 0.08, the hydrogel samples were added to the bacterial suspension and incubated in 37°C. On days 1, 3, and 5 of bacterial survival study, optical density of the bacteria and hydrogel suspensions was measured and 100 μL of suspension was evenly spread onto an agar plate (respective to the bacteria strain) and incubated in 37°C overnight. On days 2, 4, and 6 of the survival study, the colony forming units (CFU) were counted. (N=3)

2.4.2 Scanning Electron Microscopy (SEM)

SEM images were taken of hydrogel samples that were incubated in a bacterial suspension for the antimicrobial test to observe the hydrogel surface after antibacterial testing in order to visualize the bactericidal property of the biomaterial. Samples for SEM were prepared by removing the hydrogels from the bacterial suspension and washing three times with DPBS. The bacteria were then fixed onto the polymer after 2 h of submersion in 2.5 %(v/v) glutaraldehyde. The samples were again rinsed three times in DPBS and then lyophilized for 48 h. Lastly, the samples were mounted on SEM stubs, sputter coated with 6 nm of gold/palladium, and visualized using ZEISS Supra 40VP SEM.

2.5 *In vitro* biocompatibility studies

In vitro biocompatibility of the PVA hydrogels was assessed with human lung fibroblast cells (hLFBCs) (Lonza). Cells were cultured in Dulbecco's Modified Eagle Medium (DMEM) supplemented with 10% fetal bovine serum (FBS) and 1 %(v/v) penicillin/streptomycin. The hLFBCs were cultured a polystyrene tissue culture flask (Corning) and incubated at 37˚C with 5% CO_2. Cells were seeded at 1×10^4 cells/cm^2 at the bottom of a 24-well Polystyrene Tissue Culture Plate (CELLTREAT Scientific). The sterically prepared PVA hydrogels were incubated alongside the hLFBCs. The hydrogel-treated cells were incubated up to 7 days and the culture medium was replaced every 48 h.

2.5.1 Live/Dead cytotoxicity assay

Viability of the cultured human lung fibroblasts was studied using a Live/Dead™ Viability/Cytotoxicity Kit (Invitrogen) according to instruction from the manufacturer at days 1, 3 and 7 of culture. An assay solution of 0.5 μL/mL calcein-AM and 2 μL/mL ethidium homodimer-1 (EthD-1) in DPBS was used to stain cells for 20 min at 37°C. The cells were washed and subsequent fluorescent imaging was performed using an AxioObserver Z7 inverted microscope (Zeiss). The viability assay was conducted on days 1, 3 and 7 after hydrogel treatment. Live and dead cells were determined by green and red color, respectively and quantified using the ImageJ software. Cell viability was determined as the number of live cells divided by the total number of cells.

2.5.2 Actin/DAPI staining

Cell spreading on the hydrogels was visualized by fluorescent staining of F-actin microfilaments and cell nuclei to assess the morphology and spreading of the hLFBCs. After days 1, 3 and 7 of co-culture with the hydrogels, hLFBCs were fixed in 4 %(v/v) paraformaldehyde (Sigma) for 10 min, washed, permeabilized in 0.3 %(w/v) Triton X-100 (Sigma) for 10 min, washed, and then blocked with 1%(w/v) bovine serum albumin (BSA, Sigma) for 30 min. Samples were then incubated in a staining mixture of 2 μL/mL Alexa Fluor 594 phalloidin (Invitrogen) and 1 μL/mL DAPI (4′,6-diamidino-2-phenylindole, Sigma) for 20 min. After washing thrice with DPBS, fluorescent images were taken using an inverted fluorescence microscope (Zeiss Axio Observer Z7). Cell number was calculated by determining the number of cells per area of well plate.

2.5.3 PrestoBlue™ metabolic activity assay

The metabolic activity of the human lung fibroblasts was characterized at days 1, 3 and 7 post-seeding, using a PrestoBlue™ assay (Life Technologies). The assay was conducted according to the manufacturer's instructions. In summary, the cells were incubated in a solution of 10 %(v/v) PrestoBlue™ reagent in DMEM for 45 min at 37°C. The resulting fluorescence was measured at 600 nm using a Synergy HT fluorescence plate reader (BioTek).

2.6 Statistical analysis

Data was presented in the format of mean ± standard deviation (SD) (*: $P< 0.05$, **: $P< 0.01$, ***: $P< 0.001$, ****: $P< 0.0001$). One-way or two-way analysis of variance (ANOVA) test was performed for statistical analysis using GraphPad Prism 8.0.2 software.

CHAPTER III. RESULTS AND DISCUSSION

3.1 Structural characterization of elastic and tough hydrogel

The goal of this study is to engineer clinically relevant elastic, tough, and strong hydrogels to be used for the replacement of natural load-bearing tissues, such as cartilage, intervertebral disk, tendon, and others (Figure 1A). Functionally, these tissues show unique mechano-physical properties, including frequent reversible deformation upon different magnitude of forces and high load, while maintaining their structural integrity. Morphologically, the presence of hierarchical structures across multiple length scales are the underlining reason for elastic and tough mechanical properties[21]. Thus, the conventional hydrogels with chemically crosslinked molecular regimes and homogeneous structures fail to mimic the biomechanics of these tissues. Herein, to develop scaffolds resembling the biomechanics of natural load-bearing tissues, material engineering is adopted on both molecular and structural levels, to facilitate energy dissipation. Figure 1B illustrates the synthetic approach of the synthesis of the designed elastic and tough hydrogel using a two-step method. Initially, by introducing the freeze-thaw cycles on PVA solution, the resulting molecular entanglement provided an elastic restoring force, increasing the mechanical strength and viscoelastic energy dissipation capability[33]. Furthermore, the freeze-thaw cycles incorporated crystalline regimes in the molecular network, which are known to enhance mechanical strength in the hydrogel.[34, 35]

Meanwhile, exposing the freeze-thawed PVA hydrogels to the organo-inorganic ion solutions evoked structural diversity in the hydrogel morphology in terms of anisotropic porosity (Figure 1B-D). This was attributed to Hofmeister Effect, where solvation of the diffused ions inside the hydrogel determined the chemical microenvironment and stability of PVA macromolecules in the

molecular matrix, controlling the extent of molecular aggregation. Herein, sodium bicarbonate and choline bicarbonate, which have different solvation capability were chosen to control the salting out effect. Different concentration of the sodium bicarbonate and choline bicarbonate were used to control ionic solvation. For instance, ions with high solvation capability (sodium) may have interacted with water molecules, which reduced the water population around the macromolecules. Therefore, the intermolecular interactions between the macromolecules increased, facilitating nonhomogeneous distribution of the macromolecules in the hydrogel system followed by molecular aggregation induced macroscopic phase separation. Similar macroscopic phase separation in the hydrogel was also observed upon the introduction of charged molecules to the hydrogel, which replaced the hydrogen bonding interactions between water and macromolecules with stronger electrostatic interactions, triggering the molecular aggregation[36]. In this case, the use of organic and inorganic ions with different solvation capability may have controlled the extent of molecular macroscopic phase separation which results in the formation of anisotropic porous structural backbones. For instance, freeze-thawed hydrogels treated with higher concentration of choline with hydrophobic functionality showed almost an absence of porosity when compared to the hydrogel treated with inorganic ions, $NaHCO_3$ (Figure 1C). Due to the reduced solvation of hydrophobic ions (choline), a greater number of water molecules could interact with the PVA macromolecules to keep them well-solvated and uniformly distributed in the hydrogel system. Therefore, during the salting out process solely with choline bicarbonate, the well-solvated PVA molecules showed greatly reduced the pore size or almost an absence of pores. In contrast, the treatment with inorganic $NaHCO_3$, which easily gets solvated with water molecules, minimized the presence of water molecules around the PVA polymers. Thus, the less solvated PVA macromolecules caused aggregation, which results in non-homogeneity in the hydrogel structure

followed by the formation of bigger pores in hydrogel. Difference in hydrogel pore size upon treatment with different ratios of organo-inorganic salts are shown in Figure 1D**.** Overall, the salting-out mechanism using ions with different solvation capacity facilitated the molecular assembly and controlled the formation of anisotropic micro structured molecular framework of the engineered hydrogel materials.

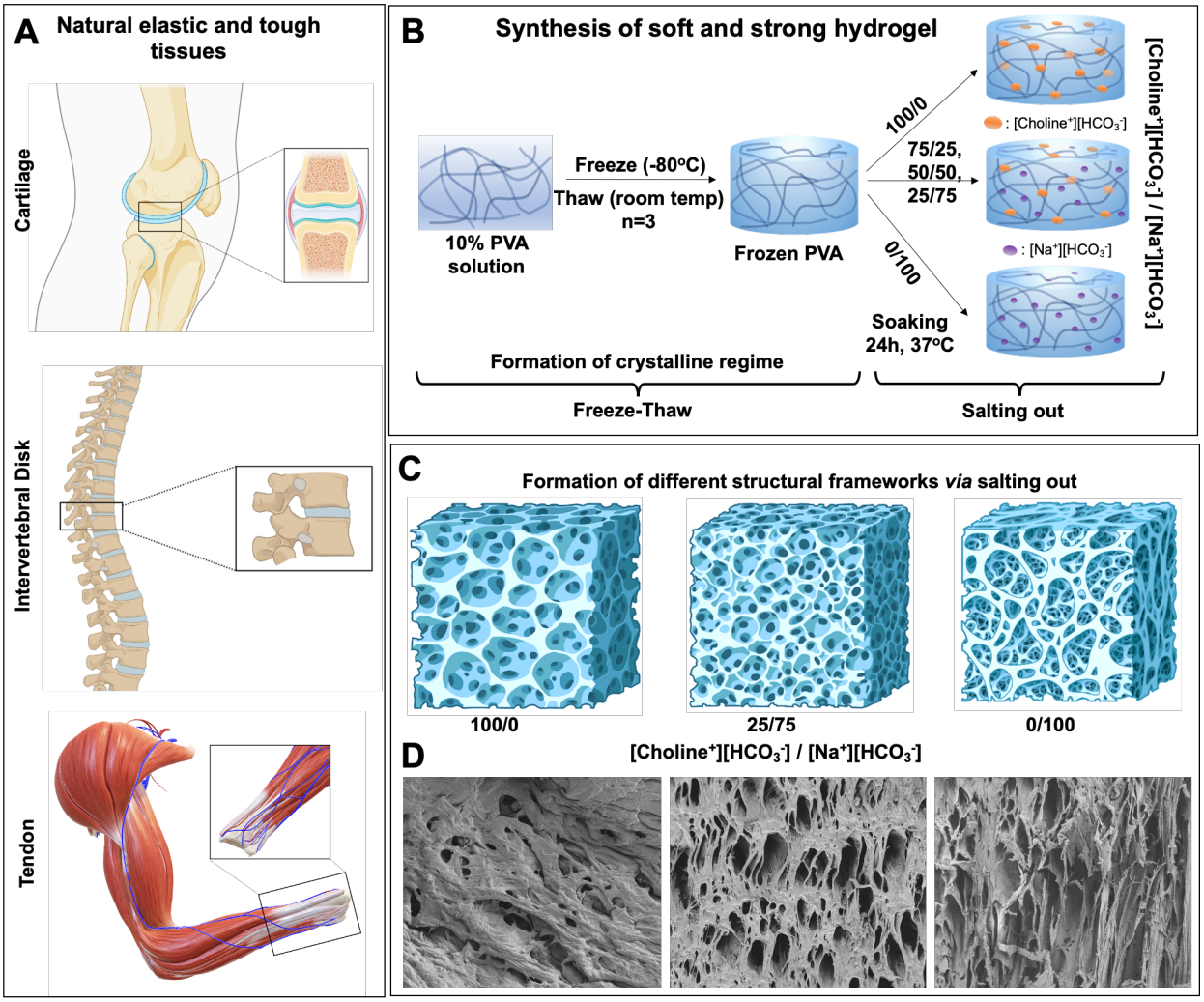

Figure 1. **Engineering elastic and tough hydrogel. (A)** Natural load bearing elastic and strong tissues. **(B)** Synthetic illustration of elastic and tough hydrogel using freeze-thaw and salting out mechanism with various concentration of %(v/v) choline bicarbonate/$NaHCO_3$ where numbers

represent percentage of choline bicarbonate to sodium bicarbonate in solution. **(C,D)** Schematically represented anisotropic microstructure molecular framework and their corresponding SEM images, formed via salting out mechanism using different ratio of organic-inorganic ion concentrations in freeze-thawed PVA hydrogel.

3.2 Mechanical Characterization of Elastic and Tough Hydrogel

3.2.1 Tensile properties

To understand the synergistic effects of freeze-thawing and salting out on the mechanical properties of the engineered hydrogel, tensile tests were performed. Figure 2A visually represents the initial and stretched PVA hydrogel treated with and without salting out. Figure 2B represents the stress-strain curve of engineered hydrogels treated with different ratios of choline bicarbonate and sodium bicarbonate salts. For instance, while ultimate strength of the PVA hydrogel without salting out effect was in the range of 10 kPa, the introduction of salting out with $NaCO_3$ improved its ultimate strength to 450 kPa (Figure 2C). The use of different ratios of organic-inorganic ions for salting out, which resulted in structural difference in the hydrogel matrix, demonstrated a different order of mechanical strength. For example, the ultimate strength for PVA hydrogels treated with 100/0, 75/25 and 0/100 %(v/v) choline bicarbonate/$NaHCO_3$ was increased from 220 ± 9, to 365 ± 10, and 478 ± 9 kPa, respectively. Increasing strength of the PVA hydrogels treated with increasing concentration of $NaHCO_3$ attributed to the salting out mediated confinement of PVA macromolecule in the solid region, which increased the localized polymer concentration of the engineered hydrogel. Similarly, with increasing $NaHCO_3$ concentrations during salting out, hydrogel stretchability increased (Figure 2D). In this case, due to the increased molecular confinement, porosity or void space in the hydrogel material increased (Figure 1C, D), which

allowed for a higher extent of deformation upon applied force. For instance, while PVA hydrogel without salting out process could stretch only 100%, treated PVA hydrogel treated hydrogel with 75/25 and 0/100 %(v/v) choline bicarbonate/$NaHCO_3$ demonstrated extensibility in the range of 150 and 180%, respectively. As expected, due to the absence of microscopic structures, PVA hydrogel without any salt treatment could bear minimal stress. However, the presence of noncovalent hydrogen bonding interactions between the PVA macromolecules supported the stretching of the engineered hydrogel. The subsequent improvement of the mechanical properties of the engineered hydrogels was attributed to the formation of microstructured molecular framework upon salting out of the freeze-thawed hydrogels.

It was found that the toughness of the engineered hydrogels increased by increasing the concentration of $NaHCO_3$ in the salting out process (Figure 2E). For instance, while PVA hydrogel without the salting out process retained a toughness of 5 ± 0.6 kJ/m^3, 100/0, 75/25, and 25/75 %(v/v) choline bicarbonate/NaHCO3-treated PVA hydrogels demonstrated toughness in the range of 160 ± 10, 280 ± 4, and 404 ± 21 kJ/m^3, respectively. In this case, the effect of molecular confinement and porosity affected the toughness of the engineered hydrogel. Meanwhile, the decrease in toughness observed in the $NaHCO_3$-treated PVA hydrogel could be due to the highly porous structure (Figure 1D), which enabled easy deformation upon applied force. Meanwhile, the absence of microstructure in the PVA hydrogels without salting out treatment showed lower Young's modulus in the range of 13 ± 2 kPa (Figure 2F). However, with increasing molecular confinement via salting out, which provided structural strength to hydrogel, Young's modulus of the engineered hydrogels increased. For instance, the Young's modulus for 100/0 was 116 ± 11 kPa which increased to 329 ± 12 kPa for the 75/25 %(v/v) choline bicarbonate/$NaHCO_3$ treated

PVA hydrogel. Meanwhile, saturation of the Young's modulus could be due to the balancing in structural strength and porosity induce easy deformability of the hydrogel.

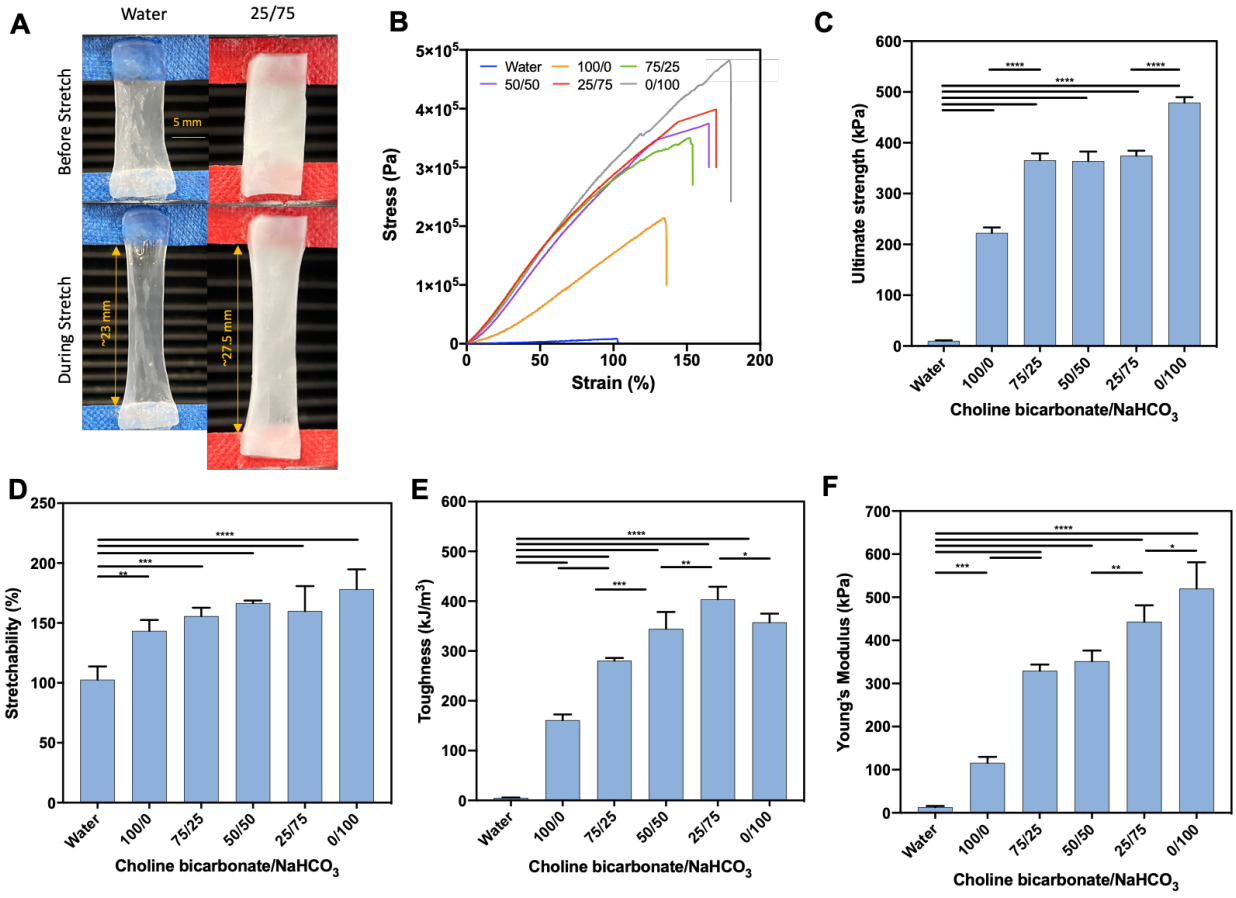

Figure 2. Tensile properties of elastic tough PVA hydrogel. (A) Representative images of pure PVA hydrogel (water) and PVA-25/75 choline bicarbonate/$NaHCO_3$ **(B)** Stress-strain curves representation **(C)** Ultimate strength **(D)** Stretchability **(E)** Toughness **(E)** Young's modulus of stretched pure PVA hydrogel (water) and PVA hydrogel made of various concentration of %(v/v) choline bicarbonate/$NaHCO_3$ (100/0, 25/75, 50/50, 25/75, 0/100), where numbers represent percentage of choline bicarbonate to sodium bicarbonate in solution. **(F)**. 10% PVA was used in all experiments. Data are represented as mean ± SD (*P < 0.1, **P < 0.01, ***P <0.001, ****P < 0.0001, N=5).

3.2.2 Compressive properties

Along with improved tensile properties, the microstructure-embedded hydrogels showed excellent compressive properties, which is essential for replacement of load-bearing tissues. To evaluate the compression modulus, engineered hydrogels with different salting out mechanisms were placed between the metal plate on an Instron mechanical tester and compressed until the gap was almost zero. Figure 3A represents the stress-strain curve for PVA hydrogels treated with different salting out process. Due to the absence of a microstructure, the PVA hydrogel without salting out possessed minimal compressive modulus, i.e., weak in nature, as compared to the engineered hydrogels developed with salting out effect (Figure 3B). For instance, PVA hydrogels formed with 100/0, 75/25, 50/50, 25/75, and 0/100 %(v/v) choline bicarbonate/$NaHCO_3$ treatment showed compressive modulus 3.3 ± 0.5 MPa, 3.5 ± 0.4 MPa, 4.0 ± 0.6 MPa, 5.1 ± 0.8 MPa , and 5.7 ± 0.4 MPa respectively. With the salting out process, the compressive modulus of the engineered hydrogels was increased significantly due to the confinement of PVA macromolecules in the structural constructs and macroscopic voids/pores. The resultant compressive modulus for our PVA salting out hydrogels, which was in the order of 3-5 MPa, was comparatively higher to the hydrogels synthesized with photocrosslinking or other processes [37-40]. Notably, obtained compressive modulus in the range of 1-5 MPa is comparable with natural load bearing tissues such as native articular cartilage and intervertebral disk, suggesting the use of engineered hydrogel as an implant for these tissues[41, 42].

Figure 3C visually represents the structure of the engineered hydrogels developed with and without salting out process. Rapture of the non-treated PVA hydrogel (water) under compressive force proved the importance of the anisotropic microstructures, which formed due to the salting out

process, to maintain the structural integrity. Structurally, natural loadbearing tissues possess high water content, high mechanical loading and flexibility in order to undergo multiple cycles of loading and unloading. Therefore, to evaluate the durability of the engineered hydrogels, cyclic compression tests were performed. Figure 3D represents different cycles of the stress-strain curve for the PVA hydrogel developed with 25/75 %(v/v) choline bicarbonate/$NaHCO_3$ treatment. Interestingly, for all the hydrogels, the energy loss was at maximum of 29 ± 0.2%, which suggests the reversible deformation of the structural constructs (Figure 3E). In addition, our material suggests lower structural deformation compared to previously reported native intervertebral disk, which has an energy loss of 41%.[43] Owing to the importance of the compressive and elastic deformation of natural load bearing tissues, mechano-physical properties of the engineered hydrogels were compared with recently developed different elastic and tough hydrogels which also involves the use of PVA with other crosslinkers or other materials with load-bearing tissue applications (Figure 3F)[37, 44-49]. Our hydrogels (PVA-CS) show a balance of high compressive strength and tensile modulus whereas other materials showed either high compressive strength and weak tensile modulus, or vice versa. Materials with varying compression and elastic moduli demonstrated their potential to be used as implants for numerous healthcare applications.

3.2.3 Swelling and degradation properties of elastic and tough hydrogel

High swelling of hydrogels is considered as one of the challenges and drawbacks for their application in medical science. Particularly for implants, increasing water content in the hydrogels induces changes in volume of the hydrogel and may reduce their mechanical strength[31]. In view of this, herein, the swelling of engineered PVA hydrogels was controlled due to presence of hydrophobic organic ions when emerged inside DPBS at 37°C (Figure 3G). Meanwhile, PVA

hydrogel synthesized without salting out process showed minimum swelling due to the absence of porous structure. However, due to the presence of hydroxyl functionality in the PVA backbone, the hydrogel material readily interacted with water molecules which lowered their mechanical integrity. Meanwhile, PVA hydrogels developed with salting out procedure, showed initial swelling due to their porous structure, which reached to an equilibrium state with no further swelling after 24 h. Reduced swelling of PVA hydrogel treated with higher concentration of choline attributed to the presence of hydrophobic chemical environment which restricted the flow of water molecules in the molecular network. For instance, while PVA hydrogel treated with 100/0 %(v/v) choline bicarbonate/$NaHCO_3$ showed non-swelling property at equilibrium condition. PVA hydrogels treated with 75/25, 50/50, 25/75, and 0/100 %(v/v) choline bicarbonate/$NaHCO_3$ treatment showed swelling ratio of 13 ± 1%, 15 ± 1%, 18 ± 2%, and 23 ± 2%, respectively, at equilibrium condition. Overall, PVA with salting out treatment showed minimal swelling whereas , PVA hydrogel without salting out treatment swelled and became mechanically weak which also indicates the absence of molecular integrity without salting out effect.

Controlling the degradation of hydrogel is another important parameter for their use as an implant to ensure longevity of the material inside the body[14]. The PVA hydrogels were immersed in collagenase type II solution, an enzyme found in bones and tendons, to test material dissociation when exposed to a physiologically relevant microenvironment. Herein, the use of choline bicarbonate and sodium bicarbonate salts minimized degradation of the engineered hydrogel while submerged inside enzymatic solution at 37°C. Furthermore, due to the presence of a hydrophobic chemical microenvironment, diffusion of the enzymatic solution inside the hydrogels was restricted, reducing the degradation of engineered hydrogels. Figure 3H demonstrated a

physiologically relevant degradation period of engineered hydrogel. PVA hydrogels developed with salting out procedure maintains a 11 ± 2.2% degradation after 7 days, whereas PVA hydrogels without ion treatment observed continued degradation up to 37 ± 0.3% after 60 days which proved that salting out enhanced PVA hydrogel's long-term structural integrity in physiological conditions.

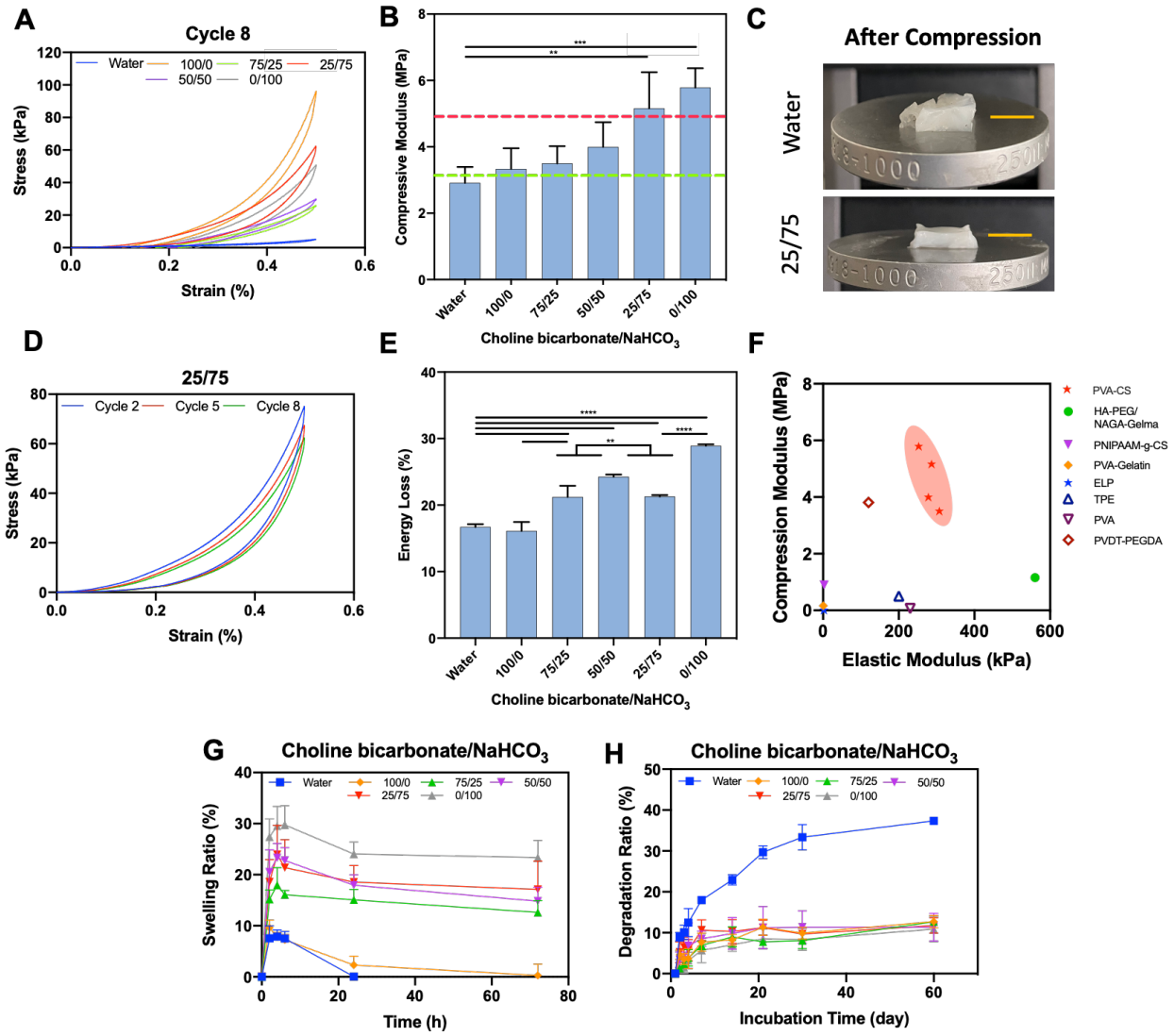

Figure 3. Load bearing, tissue mimicking biophysical properties of elastic and tough PVA hydrogel. (A) Representative stress/strain curve for cyclic test at cycle 8 and **(B)** Compressive modulus of elastic and tough PVA hydrogel with (100/0, 25/75, 50/50, 25/75, 0/100) and without

(water) various concentration of %(v/v) choline bicarbonate/$NaHCO_3$. **(C)** Representative image of pure PVA hydrogel (water) and PVA-25/75 choline bicarbonate/ $NaHCO_3$ hydrogel after compression. **(D)** Representative stress/strain curve for cyclic test on PVA-25/75 choline bicarbonate/ $NaHCO_3$ hydrogel at cycle 2,5,8 **(E)** Energy loss of all concentrations of elastic and tough PVA hydrogel. **(F)** Comparison of elastic and compressive modulus of PVA with other relevant materials. **(G)** Swelling and **(H)** Enzymatic degradation of PVA hydrogels. 10% PVA was used in all experiments. Data are represented as mean ± SD (*P < 0.1, **P < 0.01, ***P <0.001, ****P < 0.0001, N=4). Scale bar: 5mm

3.3 Antibacterial properties of elastic and tough hydrogel

To be used long-term inside the body, it is necessary for hydrogel inside the body to be biologically safe without causing infection. Implant-related infection remains as a persistent post-operative complication in clinical orthopedics, where infection occurs due to bacteria adhesion and colonization across the implant's surface.[50] Hence, numerous efforts have been investigated to develop antimicrobial hydrogels to eliminate bacterial proliferation and therefore prevent further medical complications.[51, 52] For example, bio-ionic liquids (Bio-ILs) such as choline have been investigated for their antibacterial properties. Bio-ILs have been utilized as non-toxic, naturally derived compounds developed for numerous biomedical applications such as drug delivery systems[53] and biosensors[54]. The activity of choline-based Bio-ILs and conductive hydrogels have been well-documented against Gram-positive and Gram-negative bacteria.[55, 56] Choline-based Bio-ILs have been also typically utilized as household agents and electronic waste for their antibacterial properties, but rarely for load-bearing tissue replacement/implant applications. Through

incorporating a series of different cationic and anionic liquids with PVA, we investigated the antibacterial properties of salting out PVA hydrogels.

Here, we incorporated different concentrations of choline bicarbonate/sodium bicarbonate and report the antimicrobial properties of the resulting hydrogels against Gram-positive *Staphylococcus aureus* and Gram-negative *Pseudomonas aeruginosa*. For this, we measured optical density (OD), colony forming units (CFU), as well as visual inspection of the bacteria-cultured hydrogel surface via SEM. To investigate OD, the PVA hydrogels were immersed in bacterial solution containing *S. aureus* and *P. aeruginosa* (with a control of no hydrogel treatment), where a steady decrease in OD was observed after 3 days of treatment with ion-treated hydrogels. The hydrogel containing no salting out effect (water) maintained an OD of 0.7 ± 0.1 for *P. aeruginosa* and 0.6 ± 0.02 for *S. aureus* after 5 days. By day 5 of bacterial immersion, salt-treated samples had a decrease in optical density of 0.2 ± 0.02 for *P. aeruginosa* and 0.06 ± 0.01 for *S. aureus*. The untreated *P. aeruginosa* control proliferated up to 0.4 ± 0.01 whereas the *S. aureus* control proliferated up to 0.2±0.01. These values were higher compared to ion-treated PVA, indicating that the presence of sodium bicarbonate and choline bicarbonate played a role in inhibiting bacteria growth. Bacteria viability was further examined with CFU for 6 days using the optical density assay to investigate the effect of bacteria proliferation on the material. When immersed in either *P. aeruginosa or S. aureus,* hydrogel without salt treatment grew to >1000 CFU and remained consistent with the control which only had bacteria broth. Meanwhile, all salt-treated concentrations of PVA hydrogels showed significant decrease within the course of 5 days for *S. aureus* and decreased after day 3 for *P. aeruginosa*. The results indicate that the conductive density in choline bicarbonate and sodium bicarbonate-initiated cell membrane disruption with the

ionic species. The antibacterial activity was instigated by the positive charge of the cationic group that attracted the negatively charged bacteria cell membrane, which altered the structure of the outer membrane and released cytoplasmic constituents, resulting in bacterial death.[57] In addition, the bicarbonate system consumed excess protons to cause bacterial transmembrane proton gradient, which disrupted the bacterial membrane due to its effect in controlling the pH buffer system and proton motive force of Gram-positive and Gram-negative bacteria.[57] Therefore, bicarbonate itself can regulate the innate immunity which makes it intrinsically antibacterial.

Ion-treated PVA increased the bacterial defense proved by the decreasing CFU and OD, whereas non-treated PVA hydrogel (water) was more susceptible towards bacterial proliferation. This was further explored visually when bacterial broth was sprayed directly on top of the hydrogel in agar plating to see whether bacteria can form on top or surrounding it. A more visible and larger bacteria zone was exhibited on non-treated PVA hydrogel whereas little to no bacteria zone was exhibited on the ion-treated PVA samples. Further study through SEM was performed to observe bacteria formation within the hydrogel fibers. Non-treated PVA (water) had hosted a large number of bacteria whereas ion-treated PVA had hosted little to no bacteria as shown (Fig. 5D). The ability of hydrogels to break the bacterial membrane is essential to inhibit bacterial growth, hence our material can prevent bacterial infection long-term effectively. Overall, our results showed that our elastic and tough PVA-based hydrogel has bacterial resistance against both Gram-positive and Gram-negative bacteria which is important in our application as a long-term tissue implant.

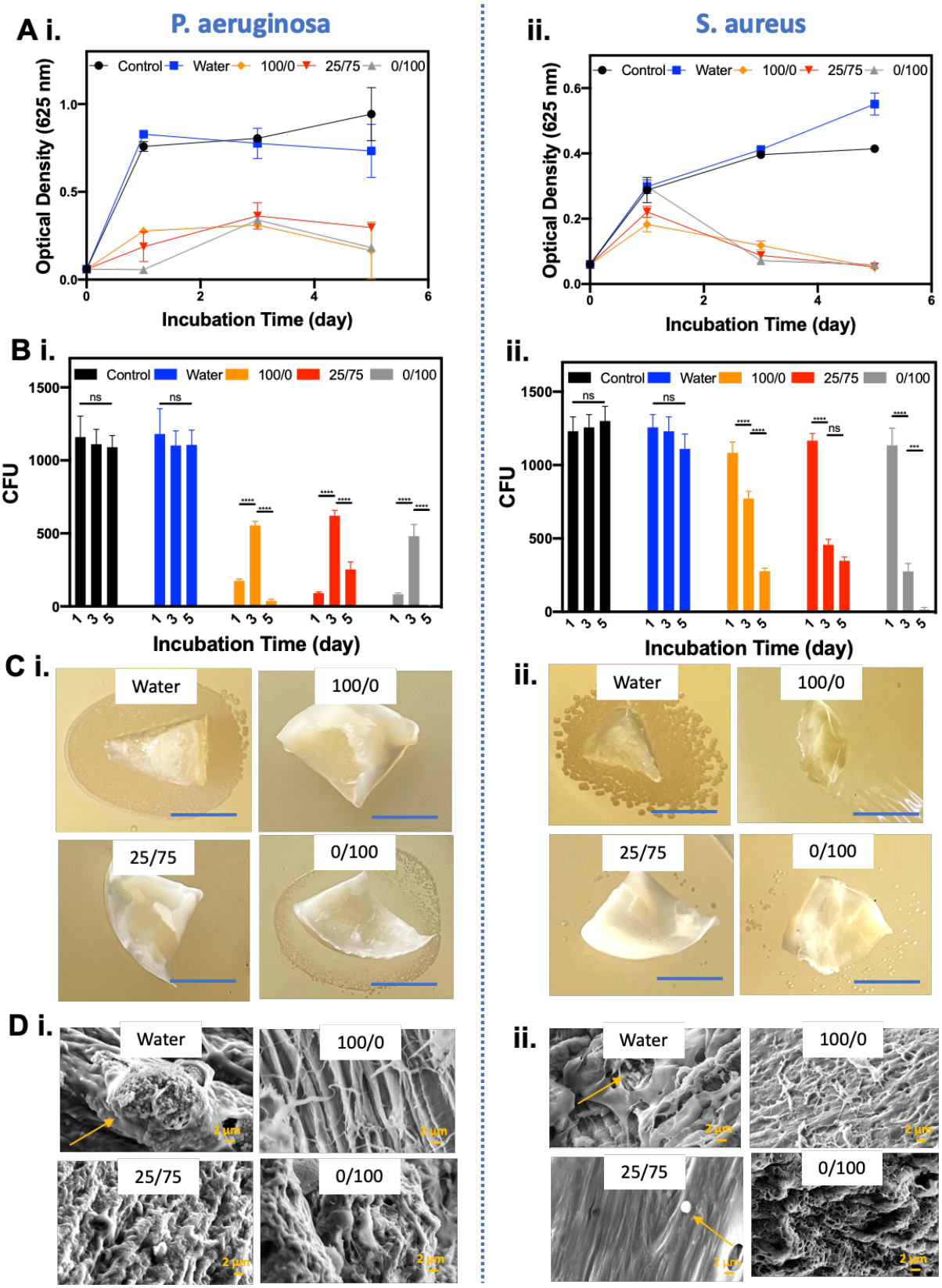
A i.
P. aeruginosa
Control
Water
100/0
25/75
0/100
Optical Density (625 nm)
Incubation Time (day)
ii.
S. aureus
B i.
CFU
ns
****
ii.
C i.
Water
100/0
25/75
0/100
ii.
D i.
2 µm
ii.

Figure 4. **Antibacterial properties of elastic and tough PVA hydrogel. (A)** Bacterial viability measured at 625 nm on **(i)** *P. aeruginosa* and **(ii)** *S. aureus* cultured at days 1,3,5 post-incubation and **(B)** Colony forming units of **(i)** *P. aeruginosa* and **(ii)** *S. aureus* after days 2,4,6 post-incubation with elastic and tough PVA hydrogels. Control was bacteria growth without presence of hydrogel. **(C)** Visual portrayal of **(i)** *P. aeruginosa* and **(ii)** S. aureus formation applied directly on top of elastic and tough PVA hydrogel after one day of incubation. Scale bar: 5 mm **(D)** SEM images of elastic tand tough PVA hydrogel after one day of incubation with **(i)** *P. aeruginosa* and **(ii)** *S. aure*us bacteria. Scale bar: 2 μm.

3.4 Biocompatibility of elastic and tough hydrogel

To demonstrate the biocompatibility of our tough hydrogel for clinical usage as a potential long-term implant, cellular biocompatibility assays were investigated using human lung fibroblast cells (hLFBCs). PVA has been previously investigated to have good biocompatibility.[58, 59] Live/dead staining was performed on ion-treated PVA hydrogels with a control of the non-treated PVA hydrogel to determine cell viability at days 1, 3 and 7 of immersion. Hydrogels with 100/0, 25/75 and 0/100 %(v/v) choline bicarbonate/$NaHCO_3$ were compared with non-treated PVA hydrogel (water) to analyze the cellular response to the modified ionic conditions. For all formulations, the hydrogels supported the viability of hLFBCs, confirming their *in vitro* biocompatibility (Figures 6A, S1A). Quantitative hLFBC viability reached >97% for all hydrogel formulations including untreated PVA hydrogel which showed the non-toxic chemical nature of PVA (Figure 6C). Our results were consistent with previous works where cell viability reached above 80% for PVA-based hydrogels.[60] The cell adhesion and proliferation on PVA with salting out treatment showed no significant difference when compared to that on the PVA control group (water), which

demonstrated the biocompatible nature of PVA. The cell morphology and spreading of hLFBCs seeded on the hydrogels was also visualized through Actin/DAPI staining (Figures 6B, S1B). The PVA hydrogel-seeded cells showed increased and healthy spreading after days 1, 3, and 7 of incubation (Figure 6D). After day 7, it was found that there was a substantial increase in spreading to 1690 ± 70 cells/mm^2 in 25/75 sample containing higher amounts of sodium bicarbonate, implying that sodium bicarbonate may promote healthy cell growth. Previous research has also suggested that soaking hydrogels into sodium bicarbonate achieved the pH value necessary for cell adhesion for 7 days, which enhanced cell adhesion and proliferation.[61] The metabolic activity of hLFBCs treated with hydrogels was also investigated using a PrestoBlue™ assay (Figure 6E). When added to the cells, the PrestoBlue™ solution becomes highly fluorescent as it turns blue/purple in color which can be detected using absorbance or fluorescent measurements. The PrestoBlue™ assay indicated that the metabolic activity of the cells increased rapidly up to 7 days post-immersion for the tested PVA hydrogel formulations with no significant difference for the control group. Hence, these studies suggest that our tough PVA hydrogels retains *in vitro* biocompatibility which deems them biologically safe for implantation inside physiological conditions.

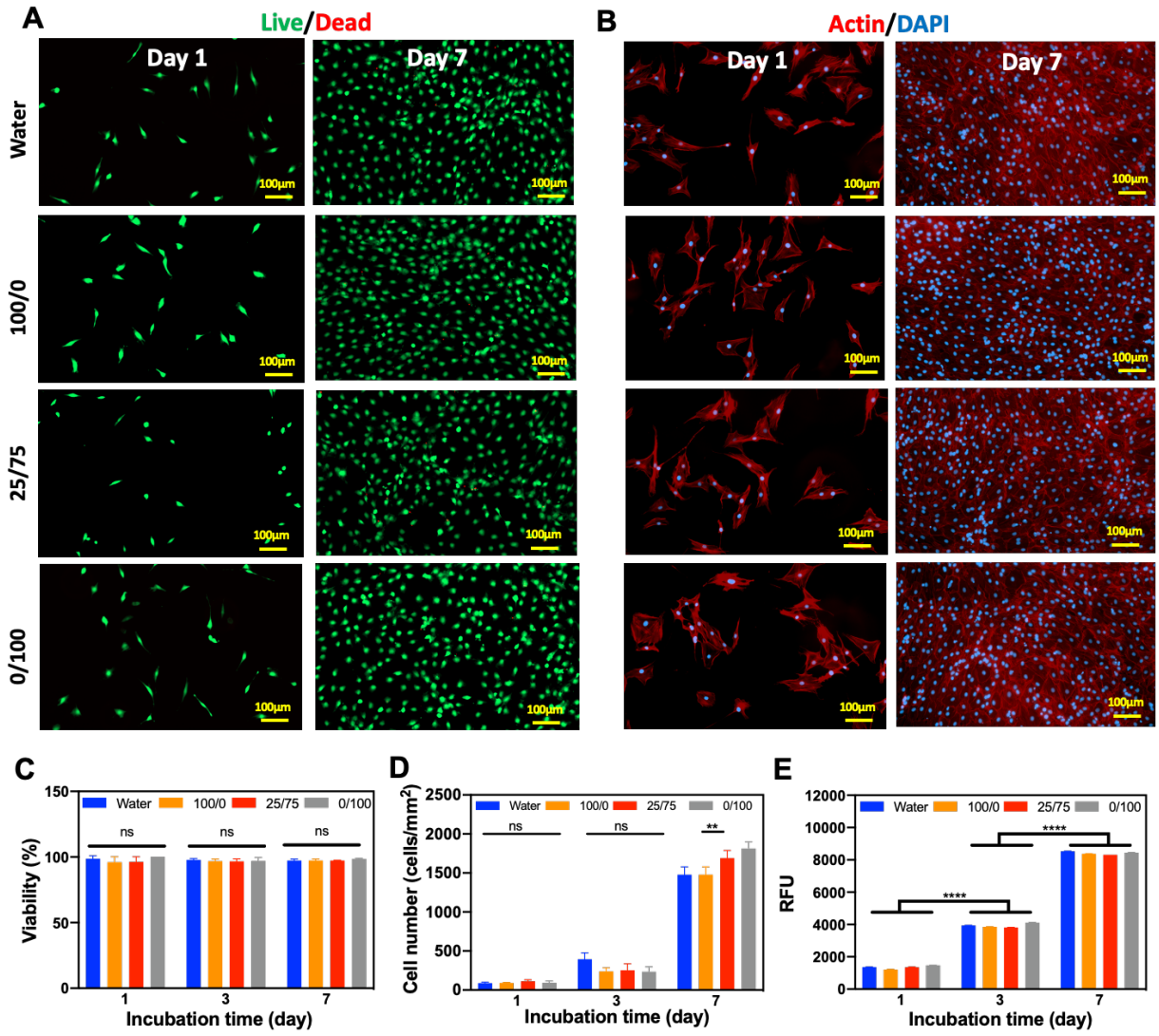

Figure 5. ***In vitro*** **biocompatibility of elastic and tough PVA hydrogel.** Representative **(A)** live/dead and **(B)** Actin/DAPI stained images of human lung fibroblast cells (hLFBCs) where elastic and tough PVA hydrogel were immersed in same wells at days 1 and 7 post seeding (scale bar: 100 μm) **(C)** Quantitative analysis of hLFBC viability at days 1, 3 and 7 post seeding **(D)** Quantitative analysis of hLFBC proliferation at days one, three and seven post seeding **(E)** Metabolic activity after hydrogel immersion after days 1, 3 and 7 using PrestoBlue assay. 10% PVA was used in all experiments. Data are represented as mean ± SD (*P < 0.1, **P < 0.01, ***P <0.001, ****P < 0.0001, N=3).

CHAPTER IV. CONCLUSION

Here we demonstrated the clinical applicability of a multifunctional hydrogel to be potentially used as an implant for load-bearing tissue. The novel hydrogel composition of PVA treated with sodium bicarbonate and choline bicarbonate organo-inorganic salts was exemplified *in vitro* to be antibacterial and biocompatible. The elastic and tough nature was achieved by tuning the hydrogels' macroscopic structure by treating PVA with the aforementioned organo-inorganic salts, which controlled and strengthened the molecular framework through a two-step process of freeze-thawing and salting out induced by the Hofmeister effect. By doing this, we observed the hydrogel's mechanical properties to mimic those of load-bearing tissues. Furthermore, the long-term stability of this biomaterial was assured by its antibacterial resistance against Gram-negative and Gram-positive strains, confirming its potential as a biomedical implant. Lastly, *in vitro* biocompatibility tests on hLFBCs also demonstrated the feasibility of safely utilizing this hydrogel in the human body, ultimately progressing the clinical translation of this biomaterial. Going forward, more work will be done with *in vivo* and *ex vivo* tests to assess its potential as a cartilage or vertebral disk implant. Overall, we believe that this approach of engineering a tough, elastic and strong hydrogel will help overcome the need for developing implants for deteriorating load-bearing biological tissues.

APPENDIX

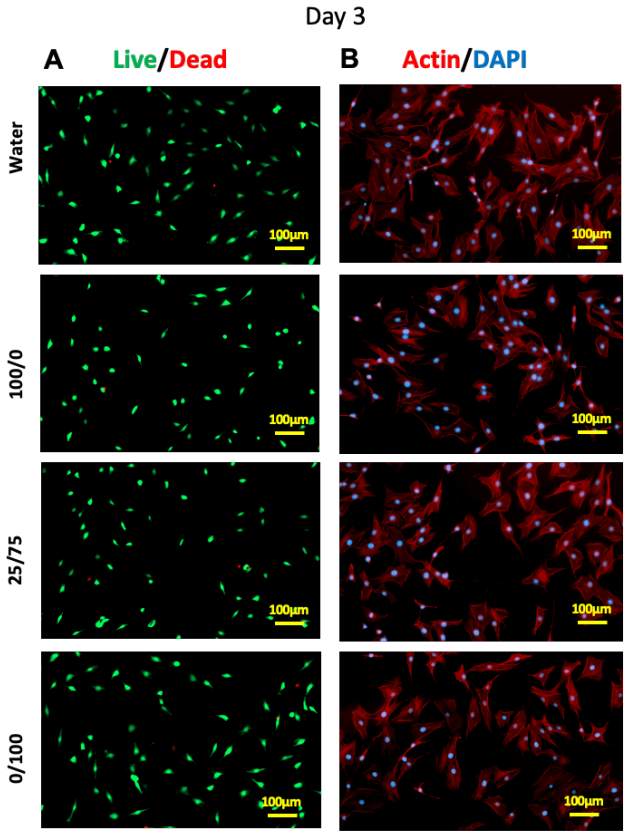

Supplementary Figure 1. (A) Live/Dead and **(B)** Actin/DAPI staining assays with human lung fibroblast cells (hLFBCs) where PVA hydrogel with (100/0, 25/75, 0/100) and without (water) %(v/v) choline bicarbonate/$NaHCO_3$ samples were immersed in same wells at day 3 post seeding (scale bar: 100 µm)

BIBLIOGRAPHY:

1. Li, J.; Mooney, D. J., Designing hydrogels for controlled drug delivery. *Nature Reviews Materials* **2016,** *1* (12), 16071.

2. Zhao, Y.; Song, S.; Ren, X.; Zhang, J.; Lin, Q.; Zhao, Y., Supramolecular Adhesive Hydrogels for Tissue Engineering Applications. *Chemical Reviews* **2022,** *122* (6), 5604-5640.

3. Liang, Y.; He, J.; Guo, B., Functional Hydrogels as Wound Dressing to Enhance Wound Healing. *ACS Nano* **2021,** *15* (8), 12687-12722.

4. Chuah, Y. J.; Peck, Y.; Lau, J. E. J.; Hee, H. T.; Wang, D.-A., Hydrogel based cartilaginous tissue regeneration: recent insights and technologies. *Biomaterials Science* **2017,** *5* (4), 613-631.

5. Zhao, W.; Jin, X.; Cong, Y.; Liu, Y.; Fu, J., Degradable natural polymer hydrogels for articular cartilage tissue engineering. *Journal of Chemical Technology & Biotechnology* **2013,** *88* (3), 327-339.

6. Yang, M.; Xiang, D.; Chen, Y.; Cui, Y.; Wang, S.; Liu, W., An Artificial PVA-BC Composite That Mimics the Biomechanical Properties and Structure of a Natural Intervertebral Disc. *Materials* **2022,** *15* (4), 1481.

7. Harmon, M. D.; Ramos, D. M.; Nithyadevi, D.; Bordett, R.; Rudraiah, S.; Nukavarapu, S. P.; Moss, I. L.; Kumbar, S. G., Growing a backbone – functional biomaterials and structures for intervertebral disc (IVD) repair and regeneration: challenges, innovations, and future directions. *Biomaterials Science* **2020,** *8* (5), 1216-1239.

8. Kim, K. T.; Lee, S. H.; Suk, K. S.; Lee, J. H.; Jeong, B. O., Biomechanical Changes of the Lumbar Segment after Total Disc Replacement : Charite(R), Prodisc(R) and Maverick(R) Using Finite Element Model Study. *J Korean Neurosurg Soc* **2010,** *47* (6), 446-453.

9. Zhang, Y. S.; Khademhosseini, A., Advances in engineering hydrogels. *Science* **2017,** *356* (6337), eaaf3627.

10. Li, X.; Sun, Q.; Li, Q.; Kawazoe, N.; Chen, G., Functional Hydrogels With Tunable Structures and Properties for Tissue Engineering Applications. *Frontiers in Chemistry* **2018,** *6*.

11. Hua, M.; Wu, S.; Ma, Y.; Zhao, Y.; Chen, Z.; Frenkel, I.; Strzalka, J.; Zhou, H.; Zhu, X.; He, X., Strong tough hydrogels via the synergy of freeze-casting and salting out. *Nature* **2021,** *590* (7847), 594-599.

12. Bashir, S.; Hina, M.; Iqbal, J.; Rajpar, A. H.; Mujtaba, M. A.; Alghamdi, N. A.; Wageh, S.; Ramesh, K.; Ramesh, S., Fundamental Concepts of Hydrogels: Synthesis, Properties, and Their Applications. *Polymers* **2020,** *12* (11), 2702.

13. Jones, L. C.; Tsao, A. K.; Topoleski, L. D. T., Orthopedic Implant Retrieval and Failure Analysis. In *Degradation of Implant Materials*, Eliaz, N., Ed. Springer New York: New York, NY, 2012; pp 393-447.

14. Sun, J.-Y.; Zhao, X.; Illeperuma, W. R. K.; Chaudhuri, O.; Oh, K. H.; Mooney, D. J.; Vlassak, J. J.; Suo, Z., Highly stretchable and tough hydrogels. *Nature* **2012,** *489* (7414), 133-136.

15. Morelle, X. P.; Illeperuma, W. R.; Tian, K.; Bai, R.; Suo, Z.; Vlassak, J. J., Highly Stretchable and Tough Hydrogels below Water Freezing Temperature. *Advanced Materials* **2018,** *30* (35), 1801541.

16. Xu, R.; Ma, S.; Lin, P.; Yu, B.; Zhou, F.; Liu, W., High Strength Astringent Hydrogels Using Protein as the Building Block for Physically Cross-linked Multi-Network. *ACS Applied Materials & Interfaces* **2018,** *10* (9), 7593-7601.

17. Bin Imran, A.; Esaki, K.; Gotoh, H.; Seki, T.; Ito, K.; Sakai, Y.; Takeoka, Y., Extremely stretchable thermosensitive hydrogels by introducing slide-ring polyrotaxane cross-linkers and ionic groups into the polymer network. *Nature Communications* **2014,** *5* (1), 5124.

18. Zheng, S. Y.; Liu, C.; Jiang, L.; Lin, J.; Qian, J.; Mayumi, K.; Wu, Z. L.; Ito, K.; Zheng, Q., Slide-Ring Cross-Links Mediated Tough Metallosupramolecular Hydrogels with Superior Self-Recoverability. *Macromolecules* **2019,** *52* (17), 6748-6755.

19. Bilici, C.; Okay, O., Shape Memory Hydrogels via Micellar Copolymerization of Acrylic Acid and n-Octadecyl Acrylate in Aqueous Media. *Macromolecules* **2013,** *46* (8), 3125-3131.

20. Maganaris, C. N.; Paul, J. P., In vivo human tendon mechanical properties. *The Journal of Physiology* **1999,** *521* (1), 307-313.

21. Zhao, X., Multi-scale multi-mechanism design of tough hydrogels: building dissipation into stretchy networks. *Soft Matter* **2014,** *10* (5), 672-687.

22. Mredha, M. T. I.; Guo, Y. Z.; Nonoyama, T.; Nakajima, T.; Kurokawa, T.; Gong, J. P., A Facile Method to Fabricate Anisotropic Hydrogels with Perfectly Aligned Hierarchical Fibrous Structures. *Advanced Materials* **2018,** *30* (9), 1704937.

23. Huang, Y.; King, D. R.; Sun, T. L.; Nonoyama, T.; Kurokawa, T.; Nakajima, T.; Gong, J. P., Energy-Dissipative Matrices Enable Synergistic Toughening in Fiber Reinforced Soft Composites. *Advanced Functional Materials* **2017,** *27* (9), 1605350.

24. King, D. R.; Sun, T. L.; Huang, Y.; Kurokawa, T.; Nonoyama, T.; Crosby, A. J.; Gong, J. P., Extremely tough composites from fabric reinforced polyampholyte hydrogels. *Materials Horizons* **2015,** *2* (6), 584-591.

25. Wei, W., Hofmeister Effects Shine in Nanoscience. *Advanced Science n/a* (n/a), 2302057.

26. Yan, G.; He, S.; Chen, G.; Ma, S.; Zeng, A.; Chen, B.; Yang, S.; Tang, X.; Sun, Y.; Xu, F.; Lin, L.; Zeng, X., Highly Flexible and Broad-Range Mechanically Tunable All-Wood Hydrogels with Nanoscale Channels via the Hofmeister Effect for Human Motion Monitoring. *Nano-Micro Letters* **2022,** *14* (1), 84.

27. Swann, J. M. G.; Bras, W.; Topham, P. D.; Howse, J. R.; Ryan, A. J., Effect of the Hofmeister Anions upon the Swelling of a Self-Assembled pH-Responsive Hydrogel. *Langmuir* **2010,** *26* (12), 10191-10197.

28. Wu, S.; Zhu, C.; He, Z.; Xue, H.; Fan, Q.; Song, Y.; Francisco, J. S.; Zeng, X. C.; Wang, J., Ion-specific ice recrystallization provides a facile approach for the fabrication of porous materials. *Nature Communications* **2017,** *8* (1), 15154.

29. Du, R.; Hu, Y.; Hübner, R.; Joswig, J.-O.; Fan, X.; Schneider, K.; Eychmüller, A., Specific ion effects directed noble metal aerogels: Versatile manipulation for electrocatalysis and beyond. *Science Advances* **2019,** *5* (5), eaaw4590.

30. Wu, S.; Hua, M.; Alsaid, Y.; Du, Y.; Ma, Y.; Zhao, Y.; Lo, C.-Y.; Wang, C.; Wu, D.; Yao, B.; Strzalka, J.; Zhou, H.; Zhu, X.; He, X., Poly(vinyl alcohol) Hydrogels with Broad-Range Tunable Mechanical Properties via the Hofmeister Effect. *Advanced Materials* **2021,** *33* (11), 2007829.

31. Qureshi, D.; Sahoo, A.; Mohanty, B.; Anis, A.; Kulikouskaya, V.; Hileuskaya, K.; Agabekov, V.; Sarkar, P.; Ray, S. S.; Maji, S.; Pal, K., Fabrication and Characterization of Poly (vinyl alcohol) and Chitosan Oligosaccharide-Based Blend Films. *Gels* **2021,** *7* (2), 55.

32. Yang, F.; Zhao, J.; Koshut, W. J.; Watt, J.; Riboh, J. C.; Gall, K.; Wiley, B. J., A Synthetic Hydrogel Composite with the Mechanical Behavior and Durability of Cartilage. *Advanced Functional Materials* **2020,** *30* (36), 2003451.

33. Hassan, C. M.; Peppas, N. A., Structure and Morphology of Freeze/Thawed PVA Hydrogels. *Macromolecules* **2000,** *33* (7), 2472-2479.

34. Adelnia, H.; Ensandoost, R.; Shebbrin Moonshi, S.; Gavgani, J. N.; Vasafi, E. I.; Ta, H. T., Freeze/thawed polyvinyl alcohol hydrogels: Present, past and future. *European Polymer Journal* **2022,** *164*, 110974.

35. Baidya, A.; Haghniaz, R.; Tom, G.; Edalati, M.; Kaneko, N.; Alizadeh, P.; Tavafoghi, M.; Khademhosseini, A.; Sheikhi, A., A Cohesive Shear-Thinning Biomaterial for Catheter-Based Minimally Invasive Therapeutics. *ACS Applied Materials & Interfaces* **2022,** *14* (38), 42852-42863.

36. Noshadi, I.; Walker, B. W.; Portillo-Lara, R.; Shirzaei Sani, E.; Gomes, N.; Aziziyan, M. R.; Annabi, N., Engineering Biodegradable and Biocompatible Bio-ionic Liquid Conjugated Hydrogels with Tunable Conductivity and Mechanical Properties. *Scientific Reports* **2017,** *7* (1), 4345.

37. Baidya, A.; Ghovvati, M.; Lu, C.; Naghsh-Nilchi, H.; Annabi, N., Designing a Nitro-Induced Sutured Biomacromolecule to Engineer Electroconductive Adhesive Hydrogels. *ACS Applied Materials & Interfaces* **2022,** *14* (44), 49483-49494.

38. Baghdasarian, S.; Saleh, B.; Baidya, A.; Kim, H.; Ghovvati, M.; Sani, E. S.; Haghniaz, R.; Madhu, S.; Kanelli, M.; Noshadi, I.; Annabi, N., Engineering a naturally derived hemostatic sealant for sealing internal organs. *Materials Today Bio* **2022,** *13*, 100199.

39. Tavafoghi, M.; Sheikhi, A.; Tutar, R.; Jahangiry, J.; Baidya, A.; Haghniaz, R.; Khademhosseini, A., Engineering Tough, Injectable, Naturally Derived, Bioadhesive Composite Hydrogels. *Advanced Healthcare Materials* **2020,** *9* (10), 1901722.

40. Yang, H.; Jekir, M. G.; Davis, M. W.; Keaveny, T. M., Effective modulus of the human intervertebral disc and its effect on vertebral bone stress. *Journal of Biomechanics* **2016,** *49* (7), 1134-1140.

41. Petitjean, N.; Canadas, P.; Royer, P.; Noël, D.; Le Floc'h, S., Cartilage biomechanics: From the basic facts to the challenges of tissue engineering. *Journal of Biomedical Materials Research Part A* **2023,** *111* (7), 1067-1089.

42. Charron, P. N.; Blatt, S. E.; McKenzie, C.; Oldinski, R. A., Dynamic mechanical response of polyvinyl alcohol-gelatin theta-gels for nucleus pulposus tissue replacement. *Biointerphases* **2017,** *12* (2).

43. Christiani, T.; Mys, K.; Dyer, K.; Kadlowec, J.; Iftode, C.; Vernengo, A. J., Using embedded alginate microparticles to tune the properties of in situ forming poly(N-isopropylacrylamide)-graft-chondroitin sulfate bioadhesive hydrogels for replacement and repair of the nucleus pulposus of the intervertebral disc. *JOR SPINE* **2021,** *4* (3), e1161.

44. Dai, X.; Zhang, Y.; Gao, L.; Bai, T.; Wang, W.; Cui, Y.; Liu, W., A Mechanically Strong, Highly Stable, Thermoplastic, and Self-Healable Supramolecular Polymer Hydrogel. *Advanced Materials* **2015,** *27* (23), 3566-3571.

45. Fischenich, K. M.; Lewis, J. T.; Bailey, T. S.; Haut Donahue, T. L., Mechanical viability of a thermoplastic elastomer hydrogel as a soft tissue replacement material. *Journal of the Mechanical Behavior of Biomedical Materials* **2018,** *79*, 341-347.

46. Zhang, Y.; Gao, H.; Luo, H.; Chen, D.; Zhou, Z.; Cao, X., High strength HA-PEG/NAGA-Gelma double network hydrogel for annulus fibrosus rupture repair. *Smart Materials in Medicine* **2022,** *3*, 128-138.

47. Holloway, J. L.; Spiller, K. L.; Lowman, A. M.; Palmese, G. R., Analysis of the in vitro swelling behavior of poly(vinyl alcohol) hydrogels in osmotic pressure solution for soft tissue replacement. *Acta Biomaterialia* **2011,** *7* (6), 2477-2482.

48. Drago, L.; Boot, W.; Dimas, K.; Malizos, K.; Hänsch, G. M.; Stuyck, J.; Gawlitta, D.; Romanò, C. L., Does Implant Coating With Antibacterial-Loaded Hydrogel Reduce Bacterial Colonization and Biofilm Formation in Vitro? *Clinical Orthopaedics and Related Research®* **2014,** *472* (11), 3311-3323.

49. Ng, V. W. L.; Chan, J. M. W.; Sardon, H.; Ono, R. J.; García, J. M.; Yang, Y. Y.; Hedrick, J. L., Antimicrobial hydrogels: A new weapon in the arsenal against multidrug-resistant infections. *Advanced Drug Delivery Reviews* **2014,** *78*, 46-62.

50. Finnegan, S., Percival, Steven L. , Clinical and Antibiofilm Efficacy of Antimicrobial Hydrogels. *Advances in Wound Care* **2015,** *4* (7), 398-406.

51. Liang, Y.; Song, Q.; Chen, Y.; Hu, C.; Zhang, S., Stretch-Induced Robust Intrinsic Antibacterial Thermoplastic Gelatin Organohydrogel for a Thermoenhanced Supercapacitor and Mono-gauge-factor Sensor. *ACS Applied Materials & Interfaces* **2023,** *15* (16), 20278-20293.

52. Ibsen, K. N.; Ma, H.; Banerjee, A.; Tanner, E. E. L.; Nangia, S.; Mitragotri, S., Mechanism of Antibacterial Activity of Choline-Based Ionic Liquids (CAGE). *ACS Biomaterials Science & Engineering* **2018,** *4* (7), 2370-2379.

53. Farha, M. A.; French, S.; Stokes, J. M.; Brown, E. D., Bicarbonate Alters Bacterial Susceptibility to Antibiotics by Targeting the Proton Motive Force. *ACS Infectious Diseases* **2018,** *4* (3), 382-390.

54. Noguchi, T.; Yamamuro, T.; Oka, M.; Kumar, P.; Kotoura, Y.; Hyonyt, S.-H.; Ikadat, Y., Poly(vinyl alcohol) hydrogel as an artificial articular cartilage: Evaluation of biocompatibility. *Journal of Applied Biomaterials* **1991,** *2* (2), 101-107.

55. Alexandre, N.; Ribeiro, J.; Gärtner, A.; Pereira, T.; Amorim, I.; Fragoso, J.; Lopes, A.; Fernandes, J.; Costa, E.; Santos-Silva, A.; Rodrigues, M.; Santos, J. D.; Maurício, A. C.; Luís, A. L., Biocompatibility and hemocompatibility of polyvinyl alcohol hydrogel used for vascular grafting—In vitro and in vivo studies. *Journal of Biomedical Materials Research Part A* **2014,** *102* (12), 4262-4275.

56. Li, Z.; Kumar, H.; Guo, C.; Shin, J.; He, X.; Lu, Q.; Bai, H.; Kim, K.; Hu, J., Development of Antifreezing, Printable, Adhesive, Tough, Biocompatible, High-Water Content Hydrogel for Versatile Applications. *ACS Applied Materials & Interfaces* **2023,** *15* (12), 16034-16045.

57. Wang, C.-X.; Ma, T.; Wang, M.-Y.; Guo, H.-Z.; Ge, X.-Y.; Zhang, Y.; Lin, Y., Facile distribution of an alkaline microenvironment improves human bone marrow mesenchymal stem cell osteogenesis on a titanium surface through the ITG/FAK/ALP pathway. *International Journal of Implant Dentistry* **2021,** *7* (1), 56.